Biosensors and Bioelectronics 225 (2023) 115088

Contents lists available at ScienceDirect

Biosensors and Bioelectronics

journal homepage: www.elsevier.com/locate/bios

Identification and detection of plasma extracellular vesicles-derived biomarkers for esophageal squamous cell carcinoma diagnosis

Qingfu Zhu [a,1], Hao Xu [a,1], Liu Huang [b,1], Jiaxin Luo [a], Hengrui Li [a], Rui Yang [a], Xiaoling Liu [c], Fei Liu [a,*]

[a] National Engineering Research Center of Ophthalmology and Optometry, Eye Hospital, Wenzhou Medical University, Wenzhou, 325027, China
[b] Department of Oncology, Tongji Hospital, Tongji Medical College, Huazhong University of Science and Technology, Wuhan, Hubei, 430030, China
[c] Center for Biological Science and Technology, Advanced Institute of Natural Sciences, Beijing Normal University at Zhuhai, Zhuhai, China

ARTICLE INFO

Keywords:
Esophageal squamous cell carcinoma
Extracellular vesicles
Proteomics
Biomarker
Diagnostics

ABSTRACT

Esophageal cancer is a malignant tumor with two-thirds of patients having a local recurrence or distant metastasis. To date, diagnostic biomarkers with high sensitivity and specificity are lacking. Extracellular vesicles (EVs) have shown their potential values as disease biomarkers as they carry specific proteins and RNAs derived from cancer cells. In this study, we investigate ESCC precision diagnostics from the insights of circulating EVs, and integrate the ultrafast EV isolation approach (EXODUS) and ELISA for fast detection and screening of ESCC patients. First, we isolate and characterize the high-purity plasma EVs with EXODUS and identify 401 proteins and 372 proteins from ESCC patient and healthy individuals, respectively. Further looking into the differentially expressed proteins (DEPs) of ESCC patients and enriched KEGG pathways, we discover EV-CD14 as a potential diagnostic biomarker for ESCC, which has been further validated as a significantly differentially expressed protein by Western Blot and immunogold labelling TEM. For fast screening and detection of ESCC towards clinical applications, we apply ELISA method to diagnose ESCC from 60 clinical samples based on circulating EV-CD14, which shows a high AUC value up to 96.0% for detection of ESCC in a test set (30 samples), and displays a high accuracy rate up to 90% for prediction of ESCC in a screening test (30 samples). Our results suggest that the circulating EV-CD14 may highly be related to the initiation and progression of ESCC, providing a novel method for the diagnosis and prognosis of ESCC towards clinical translations.

1. Introduction

Esophageal cancer is the 7th leading type of cancer and the 6th most common cause of cancer death worldwide, with approximately 572,000 new cases and 508,000 deaths in 2018 (Arnold et al., 2020). The majority of cases occurred in Asia, with an estimated 307,000 cases in China alone (Bray et al., 2018; Cao et al., 2021). In addition, more than two-thirds of patients have local recurrence or distant metastasis after surgery. Based on the histological classification, esophageal cancer can be divided into esophageal adenocarcinoma (EAC) and esophageal squamous cell carcinoma (ESCC), the latter represents over 90% of all esophageal cancers with a very low overall five-year survival rate of 10%–30% (Gu et al., 2012; Nyrén and Adami, 2009). Most patients are diagnosed during the late stages of the disease due to the lack of early symptoms, resulting in limited treatment options (Arnold et al., 2019). Even after radiofrequency ablation combined with esophageal resection, several patients still develop recurrence, resulting in a poor prognosis (Ohashi et al., 2015; Reeh et al., 2015). Endoscopy is the gold standard for the diagnosis of esophageal cancer. However, due to its high cost and invasive nature, it is not suitable for population screening (Markar et al., 2018). In addition, esophageal cancer lacks specific indicators. Hence, there is an urgent need to develop sensitive and specific biomarkers that are suitable for large-scale population screening. Investigating novel biomarkers, such as extracellular vesicles, metabolites, circulating tumor cells (CTCs) and ctDNA has recently garnered attention recent years, holding promise for advancing cancer precision diagnosis and improving patient outcomes (X. Li et al., 2021; Pei et al., 2020; Su et al., 2021).

Extracellular vesicles (EVs) are secreted from almost all types of cells and have attracted significant interest for their potential values for

* Corresponding author.
E-mail address: feiliu@wmu.edu.cn (F. Liu).
[1] These authors contributed equally to this study.

https://doi.org/10.1016/j.bios.2023.115088
Received 20 December 2022; Received in revised form 13 January 2023; Accepted 18 January 2023
Available online 20 January 2023

disease diagnosis and treatment. EVs are involved in intercellular communication by transferring proteins, nucleic acids, and lipids between donor and recipient cells through autocrine, paracrine, and endocrine mechanisms (de Jong et al., 2020; Fuentes et al., 2020). The contents of EVs reflect the physiological and pathological states of cells and tissues and hence provide clues to understanding the occurrence and development of diseases. Due to a protective lipid bilayer, proteins and nucleic acids inside EVs are resistant to degradation by circulating enzymes. For these reasons, EVs are considered promising candidate biomarkers for diseases as well as drug delivery systems (LeBleu and Kalluri, 2020; Y.-J. Li et al., 2021). Compared to other liquid biopsy analytes, such as CTCs, ctDNA, cfRNA, miRNAs, etc, EVs are more abundant in body fluids, more stable, and easier to harvest and store (Hu et al., 2021; Ramirez-Garrastacho et al., 2021). These characteristics make EVs promising cancer biomarkers (Min et al., 2021), which have been demonstrated in several studies. The expression levels of exosomal miRNA-21 were significantly higher in ESCC patients and correlated with advanced tumor classification and positive lymph node status (Tanaka et al., 2013). Also, the exosomal PCAT1 promotes ESCC cell proliferation by sponging miRNA-326 and may serve as a biomarker for ESCC (Huang et al., 2019).

A recent study demonstrated that serum exosomal miRNA-182 levels in ESCC patients before surgery were significantly higher compared to normal controls, suggesting that miRNA-182 could be a potential biomarker for ESCC (Qiu et al., 2020). Furthermore, we have previously demonstrated a metabolic marker panel based on alternations of EV metabolomic profiles to predict the risk of ESCC recurrence after surgery with high accuracy and specificity, indicating the versatile utilities of circulating EVs (Zhu et al., 2021). In this work, we aim to investigate characteristic proteins carried by plasma EVs of ESCC patients and identify potential biomarkers for ESCC detection. The EXODUS method developed in our laboratory was used for isolating high-purity EVs from plasma, which is based on negative pressure oscillation and double-coupled harmonic oscillators applied to nanomembranes for improving sample purification efficiency (Chen et al., 2021). Afterward, nanoparticle tracking analysis (NTA), transmission electron microscope (TEM), and Western blot (WB) analysis were used to characterize the isolated EVs. Proteomics analysis was then used to identify proteins associated with ESCC and GO and KEGG enrichment analysis was performed based on the differentially expressed proteins (DEPs) to identify potential biomarkers. We finally confirmed the diagnostic biomarker for ESCC through the validation of additional patient samples by immunogold-labeled electron microscopy, Western blot, and enzyme-linked immunosorbent assay (ELISA). We also analyzed the relationship between EV proteins and postoperative recurrence in ESCC patients.

2. Material and methods

2.1. Ethics approval and patient recruitment

All plasma samples used in this study were obtained from Tongji Hospital in the Tongji Medical College at Hua Zhong University of Science and Technology (Wuhan, China) and were approved by the ethics committee. A dedicated clinical expert approved the sample collection from each patient. Written consent was obtained from each patient. For proteomic study, total 8 samples were applied including 2 healthy control samples pooled from 8 individuals, and 6 ESCC samples pooled from 24 individuals. For ELISA analysis, 60 clinical samples were applied including 20 healthy controls and 40 ESCC individuals.. The pathological stage was assessed based on the Union for International Cancer Control (UICC) Tumor-Node-Metastasis (TNM) staging system. Whole blood samples were collected in vacuum pro-coagulation tubes (BD, USA) from ESCC patients and healthy individuals before surgery. The plasma samples were centrifuged at 3000×*g* for 15 min (4 °C, Rotor S-4-72, Centrifuge 5804 R, Eppendorf AG, Hamburg, Germany) to remove cell debris. All plasma samples were aliquoted and stored at −80 °C for subsequent EVs isolation.

2.2. Extracellular vesicle isolation

EVs were isolated from plasma samples using the EXODUS. Before isolation, 200 μL plasma samples were diluted with phosphate-buffered saline (PBS, filtered through a 0.22 μm filter) to a final volume of 10 mL and then filtered with a 0.22 μm membrane filter (FPE-204-013, JET BIOFIL, Guangzhou, China). Subsequently, the 10 mL centrifugation tube was placed into the EXODUS to automatically isolate EVs.

2.3. Nanoparticle tracking analysis (NTA)

The size distribution and concentration of the plasma EVs were analyzed using the NanoSight NS300 instrument (Malvern, UK). According to the manufacturer's recommendation, EVs were diluted in 1 mL PBS to attain a suitable particle number per frame. Using a micropump to eject the sample, each sample was measured at least 3 times with a capture time of 30 s. The Brownian movements of EVs were subjected to a laser light source (488 nm laser) and were recorded by a camera (camera level, 15). NTA settings were optimized and maintained constant for all samples.

2.4. Western blot (WB)

The Qubit assay (Invitrogen, USA) was used to quantitate the protein amounts of EVs for Western blot analysis. EVs were then lysed with loading buffer (P0015L, Beyotime Biotechnology, and Shanghai, China) and denatured at 100 °C for 10 min. Next, 30 μg protein from each sample was separated in a 10% sodium dodecyl sulfate-polyacrylamide gel (SDS-PAGE) and transferred onto a polyvinylidene fluoride (PVDF) blotting membrane (10600023, GE Healthcare Life Science, Freiburg, Germany). After blocking with 5% skim milk, the membranes were incubated with primary antibodies, including Alix, HSP90, CD81, CD9, and Calnexin overnight. After washing the membranes with 1 × PBST for 10 min 3 times, the membranes were incubated with a secondary antibody for 1 h at room temperature. The membrane was washed three more times, and then enhanced chemiluminescence was measured using the JS-M8 luminescence image analyzer (JS-M8, Pei Qing Science & Technology, and Shanghai, China).

2.5. Transmission electron microscope (TEM) and immunogold labelling

A 20 μL of EV sample was mixed with an equal volume of 4% paraformaldehyde and then fixed onto a 200-mesh carbon-coated copper grid (BZ11022a, Beijing Zhongjingkeyi Technology Co., Ltd., Beijing, China) for 30 min at room temperature for transmission electron microscopy. Excess PFA was carefully washed using ultrapure water. Next, the EVs were negatively stained with uranyl acetate (2%) for 30 s and the excess stain was removed with ultrapure water. Finally, EV images were captured using a transmission electron microscope (Helios Nanolab DualBeam, FEI, USA) after the grids were dried.

For immunogold labelling TEM analysis, the fixed EVs on grids were blocked with 0.1% bovine serum albumin (BSA) for 10 min first, which were then incubated with anti-CD14 antibodies (Abcam) using a dilution ratio of 1:50 for 2 h at 4 °C. After extensive washes, the copper grids were incubated with gold-labeled second antibody (gold particle size was 10 nm, G3779, Sigma), and then imaged with a transmission electron microscope (Helios Nanolab DualBeam, FEI, USA).

2.6. Liquid chromatography-mass spectrometry (LC-MS) analysis

In this study, protein extraction, enzyme digestion, and liquid chromatography-mass spectrometry tandem analysis were quantitatively used to study the proteome of the samples. In brief, after

enzymatic hydrolysis by trypsin, proteins carried on EVs were decomposed into peptides with different size, which were then separated using liquid chromatography with the EASY-nLC 1200 ultra-high-performance liquid phase system. The mobile phase A was an aqueous solution containing 0.1% formic acid and 2% acetonitrile, and the mobile phase B is an aqueous solution containing 0.1% formic acid and 90% acetonitrile. The flow rate was maintained at 500 nL/min. The separated peptides were injected into an NSI ion source and then analyzed by Orbitrap Exploris™ 480 mass spectrometry with high resolution. The source voltage was set to 2.3 kV. The data acquisition mode was obtained using a data-dependent scan (DDA) program, and the same method was used for the secondary mass spectrometry. The mass spectrometry data obtained was retrieved by Proteome Discoverer (v2.4.1.15). The identification protein must contain at least one unique peptide.

2.7. Bioinformatics analysis

To probe into the functional role of proteins in the pathogenesis of ESCC, the characteristic proteins identified in ESCC were subjected to bioinformatics analysis to explore their functional roles. For this purpose, we conducted following biological analysis including differential analysis, enrichment analysis such as KEGG (Kyoto Encyclopedia of Genes and Genomes) pathway analysis and GO (Gene Ontology) analysis based on the differentially expressed proteins. We also constructed the network map based on the identified differential expressed proteins using string database (https://cn.string-db.org/).

2.8. Enzyme-linked immunosorbent assay (ELISA)

ELISA was conducted to evaluate the expression level of CD14 in plasma extracellular vesicles. Concentrations of CD14 in each sample (100 μL) were determined according to the manufacturer's instructions (CAMILO, Nanjing, China). The reaction was detected with a microplate reader (450 nm) (SpectraMax iD3, Molecular Devices). The limit of detection (LOD) was calculated based on the calibration curve by the equation: LOD = 3.3 σ/S, where σ is the standard deviation of the response, and the S is the slope of the calibration curve.

2.9. Statistical analysis

Graph Pad Prism version 8.0 was used for graphical representation and statistical analyses. Results were presented as the mean ± standard deviation. The number of experimental replicates is represented in Fig. legends. Differences between the samples were compared using an unpaired *t*-test. $P < 0.05$ was considered statistically significant.

3. Results and discussions

ESCC is a global disease that is characterized by local invasion, early metastasis, and drug resistance. There are currently no effective non-invasive biomarkers for the diagnosis of ESCC. Hence, non-invasive biomarkers are urgently needed to effectively diagnose ESCC during the early stages and distinguish between postoperative recurrence and non-recurrence. The previous studies have mainly focused on the diagnostic ability of exosome RNAs (Jiao et al., 2020; Li et al., 2022), and overlooked the potential value of the exosome protein components. Proteins directly affect cellular function, thus it is necessary to study the protein components of plasma EVs. We obtained plasma samples from patients with ESCC for proteomics analysis. We successfully isolated EVs from the plasma of ESCC patients and healthy controls using the EXODUS, which is an EV separation and purification device developed in our laboratory. These EVs were then characterized by TEM, NTA, and WB to determine the high purity of the isolated EVs. Subsequently, we performed a comprehensive proteomics analysis of these EVs based on 4D Label-free proteomics.

3.1. Workflow for the isolation and analysis of plasma EVs

In this study, we identified biomarkers in esophageal squamous cell carcinoma using EV protein products. Fig. 1 represents the schematic diagram of the workflow. The clinical plasma samples were obtained, which included ESCC patients (recrudescent and non-recrudescent) and healthy controls (Fig. 1A). As described in Fig. 1B, tumor cells are known to secrete EVs into the blood circulation, hence, we decided to collect plasma samples from patients on their first visit to the hospital (Fig. 1C). These patients underwent resection of esophageal cancer after diagnosis and were followed up for two years after surgery. We used the EXODUS device to isolate EVs which were subsequently analyzed using downstream 4D Label-free proteomics (Fig. 1D). Related proteins were identified and analyzed by mass spectrometry (Fig. 1E and F). After additional analysis, the differential expressed protein was identified and evaluated as the potential biomarker for ESCC diagnosis (Fig. 1G).

3.2. Characterization of EVs isolated from plasma

As shown in Fig. S1, we characterized the size, morphology, and protein expression of EVs. We performed the NTA analysis to determine the size distribution of EVs among the patient and healthy groups. The results showed that EVs in both groups were between 30 and 200 nm in diameter and were present as smooth unimodal curves (Fig. S1A). There were no significant differences between the EVs from healthy controls and ESCC patients in the mean diameter and size distribution (Fig. S1A). The total number of particles in the healthy control group was lower compared to the ESCC patient group shown in Fig. S1B ($p < 0.001$, *t*-test, two-tailed). We then used the Western blot to verify the isolated EVs according to MISEV 2018 guidelines (Théry et al., 2018). The classical trans-membrane protein CD81 and CD9, the intramembrane protein HSP90, and Alix were present in all samples while the negative control Calnexin was not detected (Fig. S1C). TEM images show the typical cup morphology of EVs (Fig. S1D).

3.3. Label-free proteomics for EV protein profiling

We used 4D Label-free proteomics to analyze and identify EV proteins from ESCC patients and healthy controls. A total of 419 unique proteins were identified in circulating EVs. Among them, 372 and 401 proteins were identified in healthy controls and ESCC patients respectively (Fig. 2A). Based on the differential expression threshold ($p < 0.05$ and $FC > 1.2$), 36 differentially expressed proteins (DEPs) in ESCC EVs were identified and are shown in the volcano plot (Fig. 2B), of which, 14 proteins were up-regulated and 22 proteins were down-regulated (Table S1). Additionally, the identified EV proteins were significantly different between ESCC patients and healthy controls (Fig. 2C).

We performed GO and KEGG enrichment analysis to understand the functional significance of the DEPs, while the enrichment level of the DEPs was assessed using Fisher's exact test (Fig. 2D and E). The GO enrichment analysis results were classified into three main sections: Cellular Component (CC), Molecular Function (MF), and Biological Process (BP). As shown in Fig. 2D, for CC, the upregulated proteins were significantly enriched in EVs, and the downregulated proteins were primarily enriched in the platelet alpha granule lumen. For MF, the upregulated proteins were mainly enriched for the hemoglobin and oxygen-binding pathway. It is well known that hypoxia is an indicator of malignant tumor growth and can reflect the high proliferation of tumor cells in the tumor microenvironment, as well as the relative deficiency of oxygen induced by the higher proliferation capacity of tumor cells. In addition, hypoxia in the solid tumor is associated with increased tumor aggressiveness and poor prognosis. It has been demonstrated that a hypoxic microenvironment can promote EV release from tumor tissue to meet more complex cell-to-cell communication needs (He et al., 2022; Kumar and Deep, 2020). In the peripheral blood, molecules associated with oxygen transport are actively expressed (Chae et al., 2016;

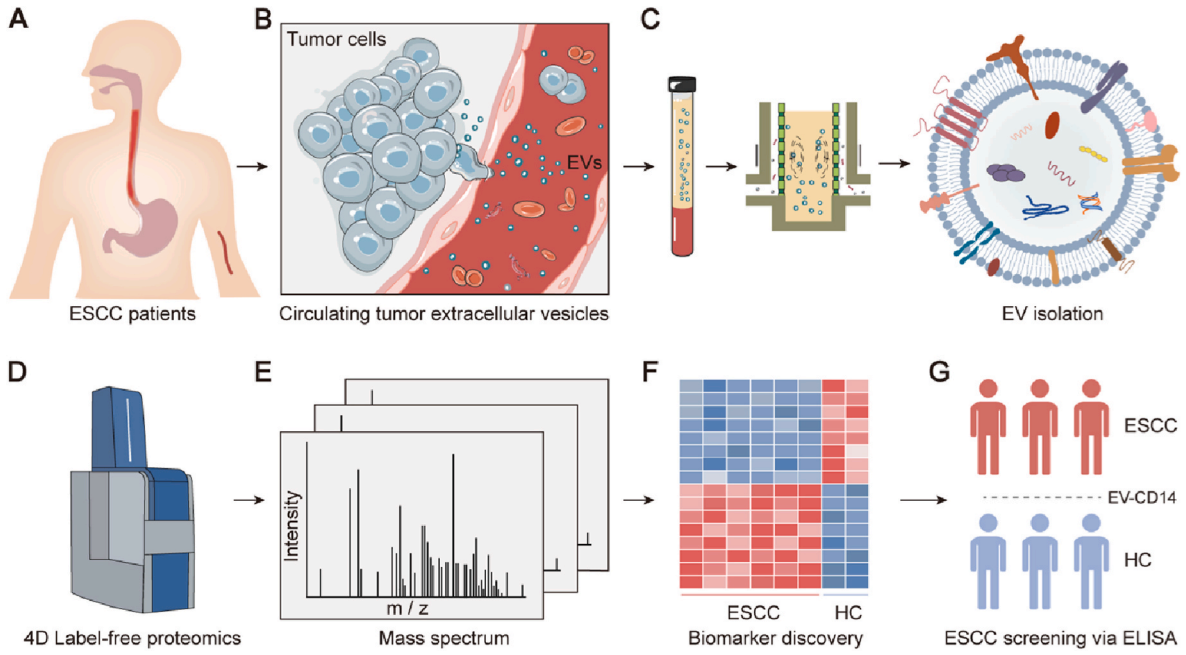

Fig. 1. Schematic illustration to identify plasma EV biomarkers in esophageal squamous cell carcinoma. (A) Patients were recruited based on clinical information. (B) Tumor cells secrete EVs into blood circulation. (C) Collection of plasma samples and EV isolation. (D) Downstream analysis of EVs using 4D Label-free proteomics, and (E) mass spectrometry. (F) Differential analysis for discovery of ESCC protein marker. (G) Fast screening and detection of ESCC based on circulating EV-CD14 via ELISA.

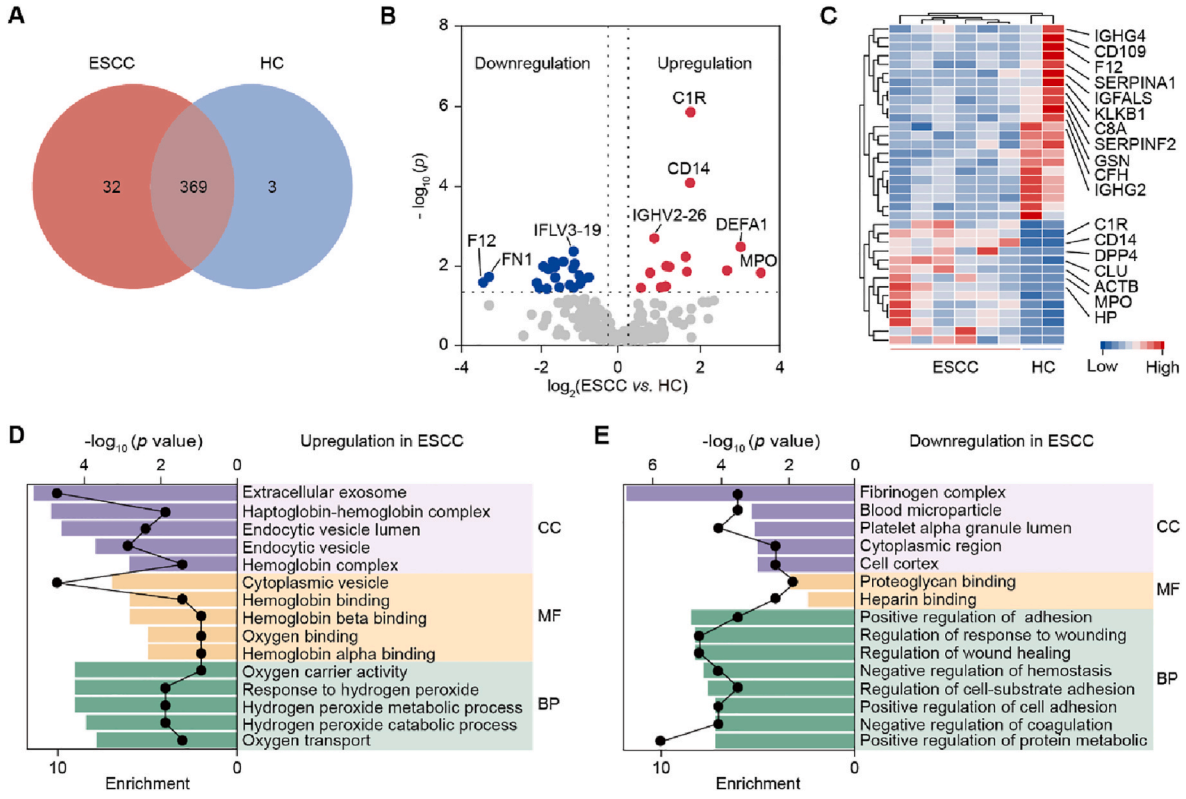

Fig. 2. Analysis of DEPs obtained from ESCC patients and healthy controls. (A) Venn plot showing the common and unique proteins from ESCC patients and healthy controls. (B) Volcano plot showing DEPs in ESCC. A false-discovery rate $P < 0.05$ and a fold change (FC) > 1.2 were used to identify proteins that were increased (red) and decreased (blue). Proteins showing no significant differences are shown in Gray. (C) Heat map showing the differences in the DEPs from ESCC patients and healthy controls. GO enrichment analysis of (D) upregulated DEPs and (E) downregulated DEPs in the cellular component (CC), molecular function (MF), and biological process (BP).

Thienpont et al., 2016), while the downregulated proteins are enriched in proteoglycan binding. For BP, the upregulated proteins were significantly involved in oxygen carrier activity and hydrogen peroxide-related pathways. It is believed that hydrogen peroxide is an intermediate product of cellular oxygen metabolism. A large amount of hydrogen peroxide is produced in cancer cells, which can transform cells into a malignant phenotype and maintain the malignant phenotype of tumor cells. Previous studies have shown that hydrogen peroxide helps tumor cells to infiltrate and metastasize to other tissues (Martínez-Reyes and Chandel, 2021). The downregulated proteins were mainly involved in the regulation of cell adhesion, which may be related to the decreased adhesion and distant metastasis of cancer cells in the tumor microenvironment. In addition, the adhesion ability of tumor cells is lower compared to normal cells, which may be related to the lower expression of intercellular adhesion molecules or the increase of intercellular electrostatic rejection. This can help the separation and shedding of tumor cells from the primary tumor, creating conditions for tumor metastasis. It has been reported that the plasma EVs derived from patients with invasive breast cancer can drive the invasive ability of non-invasive breast cancer cells, in which the invasive ability was mediated by the Focal Adhesion Kinase signaling pathway (Jordan, 2020). Another study reported that exosomes released by melanoma cells can promote tumor cell adhesion through the release of nerve growth factor receptors, thereby enhancing tumor metastasis in lymph nodes (García-Silva et al., 2021). All these studies demonstrated the occurrence and development of a tumor is a dynamic process involving adhesion proteins.

Regarding KEGG enrichment analysis (Fig. S2), our results showed that the upregulated proteins were enriched for transcriptional dysregulation in cancer. Dysregulation of transcription often occurs in the cancer transcriptome. The abnormal transcription results in proteins that may act as cancer-specific proteins, to promote tumor progression. These could be potential candidate biomarkers. Similarly, tumor antigens induced by RNA dysregulation may also be new immunotherapy targets that need to be explored (Pan et al., 2021). As for the downregulated proteins, they were mainly enriched for complement and

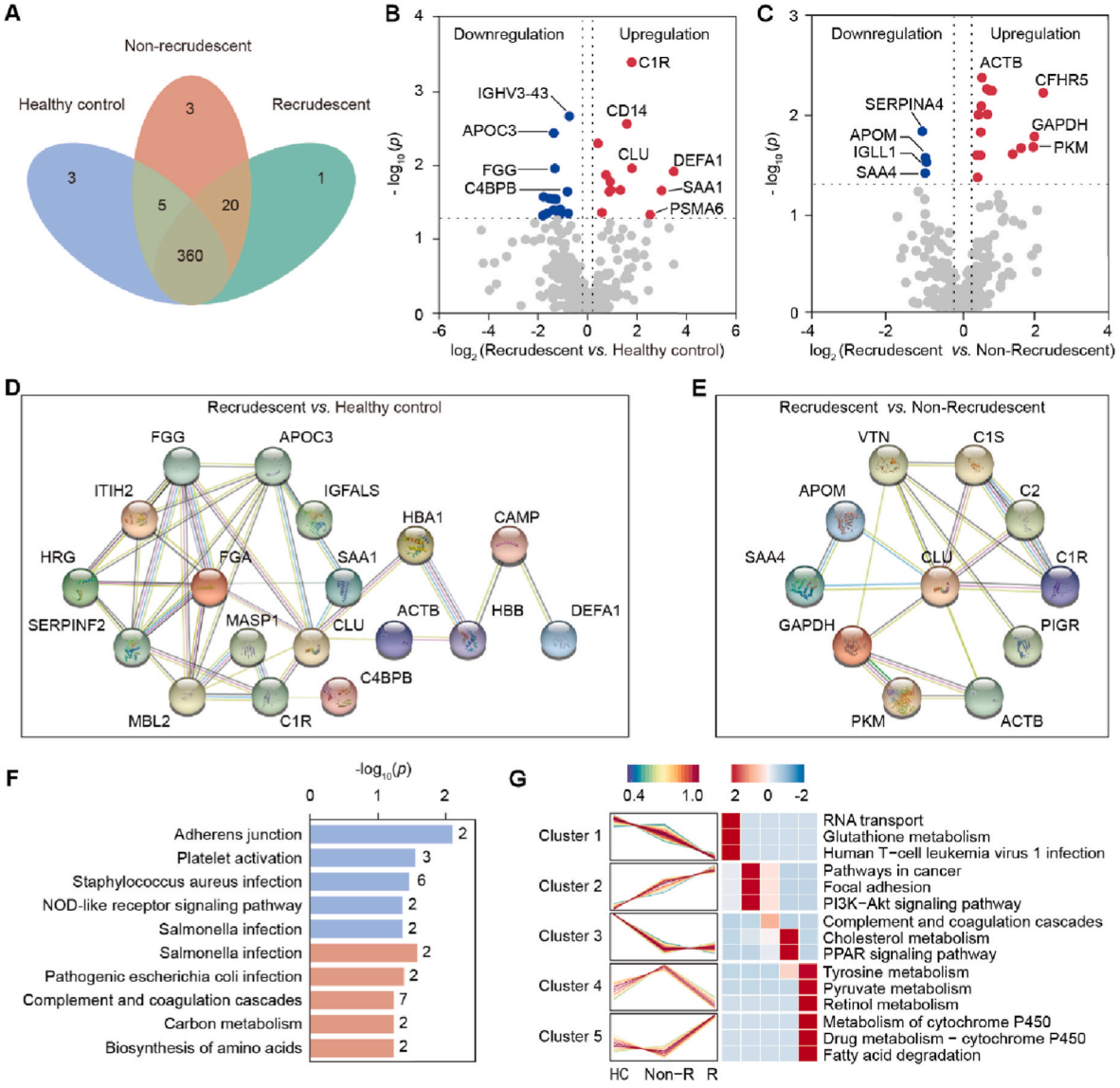

Fig. 3. DEPs in recrudescent patients versus non-recrudescent patients and healthy controls. (A) The Venn diagram shows the common and unique proteins for the different groups: healthy control, non-recrudescent, and recrudescent group. Volcano plot of the differential expressed proteins in the (B) recrudescent patients compared to the healthy controls and (C) non-recrudescent patients. The X-axis is folded change, while the y-axis denotes the p-value. (D), (E) Protein-protein interaction (PPI) network of the DEPs. (F) KEGG enrichment analysis of DEPs. Blue: R vs. HC. Orange: R vs. Non-R. (G) Expression patterns of EV proteins across the three sample groups. Proteins were classified into five clusters based on differential expression patterns. Non-R: non-recrudescent, R: recrudescent.

coagulation cascades. Cancer patients are generally in a hypercoagulable state, and excess platelets have been associated with tumor proliferation and spread (Labelle et al., 2011). High platelet levels could also promote cancer-related thromboembolism that leads to death in patients. However, complement is not harmful but may be important for antitumor immunity (Lu et al., 2020). The release of activated platelet PDGFB could help maintain the tumor blood vessel barrier to inhibit the proliferation of tumor cells (Zhang et al., 2020). The DEPs are listed in Table S1. Overall, the GO and KEGG functional enrichment analysis showed that DEPs were primarily involved in tumor cell growth, proliferation, and metastasis. These proteins may be studied as potential biomarkers for ESCC diagnosis.

3.4. Proteins associated with recurrence of ESCC after surgery

ESCC patients were divided into the recurrence group and non-recurrence group based on whether recurrence occurred within 2 years after surgery. The Venn diagram shows the overall characteristics of the three groups (Fig. 3A). Based on $P < 0.05$ and $FC > 1.2$, 27 DEPs were identified from the recurrence group and the healthy control group, and 17 DEPs were identified from the recurrence group and the non-recurrence group. A volcano plot was used to show the differentially expressed proteins in the two groups respectively. (Fig. 3B, recrudescent patients versus healthy controls; Fig. 3C: recrudescent patients versus non-recrudescent patients). We then used the STRING database (https://cn.string-db.org/) to construct the PPI network with the differential proteins of each group (Fig. 3D and E). Through network analysis and functional experiments, it has been reported that FN1 was a downstream protein of SATB1, and played a role in the proliferation, survival, and invasion of esophageal cancer cells (Song et al., 2017). Another study based on public data suggested that MPO is present in all differential modules constructed and may be a key factor for ESCC. These results confirm that DEPs we identified may play an important role in ESCC and may be a great resource for diagnostic biomarkers for ESCC.

The KEGG pathway analysis of the DEPs was primarily enriched for adherence junction, complement and coagulation cascades, and bacterial infections (Fig. 3F). We hypothesized that ESCC patients who were more susceptible to bacterial infection had a higher risk of recurrence after surgery. In addition, the over-activation of complement and clotting pathways significantly affects the prognosis of ESCC patients. Based on the different expression patterns, we classified the proteins into five clusters (Fig. 3G). Cluster 2 represents a group of proteins that gradually increased in protein levels from the healthy control group to the recurrence patient group. Functions of these proteins were mainly enriched for cancer-related pathways, including focal adhesion and PI3K/Akt signaling pathway. Previous studies have confirmed the role of the PI3K/Akt pathway in promoting cancer metastasis. It has been demonstrated that rat adrenal pheochromocytoma cells treated with exosomes derived from adipose mesenchymal stem cells had increased proliferation and migration and reduced apoptosis (Xie et al., 2021). Similarly, a recent study demonstrated that exosomes promoted the malignant behavior of CRC cells by activating the PI3K/Akt/mTOR pathway (Xu et al., 2020). These results suggest that PI3K/Akt pathway plays an important role in the progression of ESCC, especially in patients with poor prognosis.

3.5. ESCC-associated EV biomarkers

First, we observed that CD14 was significantly overexpressed in the plasma of ESCC patients (Fig. S3A and B) compared to healthy controls. This was further confirmed with Kaplan-Meier Plotter, which suggested that patients with high gene expression levels of CD14 had shorter overall survival compared to the lower controls (Fig. S3C, $p = 0.017$). CD14 is present in a membrane-anchored form and is involved in tumor immunity. A recent study showed that patients with melanoma Patients express high levels of CD14 in plasma small extracellular vesicles (Paolino et al., 2021). Another study showed that patients with low SMA who developed recurrent colorectal cancer had higher levels of CD14 expression compared to those who did not. A previous study found that a subset of bladder cancer tumor cells with high CD14 expression was able to secrete more inflammatory cytokines, such as IL6, IL8, M-CSF, VEGF-A, FGF-2, etc, and increased tumor growth (Cheah et al., 2015). These studies have demonstrated that CD14 may play an important role in tumor progression and could serve as a potential diagnostic biomarker.

We then explored whether the differential CD14 can be harnessed as markers to distinguish ESCC and healthy controls. We first performed a Western blot and immunogold labeled TEM to validate the differential expression of EV related CD14 between ESCC and healthy individuals, and found that the EVs from ESCC patients had more CD14 molecules (Fig. 4A and B). Furthermore, we performed enzyme-linked immunosorbent assay (ELISA) analysis to screen and detection of ESCC from 60 clinical samples to validate the diagnostic efficacy of EV-CD14. Firstly, the total samples were randomly divided into two groups: the test set ($n = 30$) and the screening test set ($n = 30$). For the test set, we established the standard curve of ELISA to discover ESCC patients based on differential CD14 (Fig. 4C), and confirmed that the expression levels of CD14 in EVs of ESCC patients were significantly higher than that of healthy controls with a p-value < 0.001 (Fig. 4D). The diagnostic contribution of CD14 is shown in Receiver Operating Characteristic Curve (Fig. 4E). The area under the curve (AUC) value for CD14 is 0.96, with the sensitivity and specificity values of 0.95 and 0.90, respectively. Hence, high levels of CD14 carried on circulating EVs can be a biosignature for the diagnosis of ESCC.

The 95% confidence intervals for CD14 expression level of ESCC patients in test set were between 1.594 and 2.558 ng/mL plasma, while those of healthy controls were 0.777–1.284 ng/mL plasma. The limit of detection (LOD) of EV-CD14 was calculated to be 0.127 ng/mL based on the calibration curve with standard samples in PBS buffer. Since EV particles were purified and stored in PBS buffer, and the detected levels of EV-CD14 in clinical samples were far greater than LOD, the measured values were considered reliable and can reflect the real difference between patients and healthy individuals. For fast screening, we set a cutoff of EV-CD14 expression level at 1.300 ng/mL (the optimal threshold in ROC curve) for ESCC detection. As shown in Fig. 4F, EV-CD14 leads to a good diagnostic prediction of ESCC, with an accuracy up to 90% from 30 samples, indicating its great potentials for precisely diagnosing ESCC patients towards clinical applications. Furthermore, we have compared our method based on ELISA detection of EV-CD14 to the existing methods for ESCC diagnosis, and the comparison data in terms of AUC, sensitivity, specificity, non-invasiveness and clinical screening ability was summarized in Table 1. The data shows that our method has the highest sensitivity up to 0.95, and a relatively high specificity of 0.90 comparted to other methods. Additionally, based on the selected cut-off value of EV-CD14, we have performed ESCC screening with a high accuracy up to 90%, which is higher than all the listed existing methods. In summary, our method for ESCC diagnosis is highly precision and easy-to-perform, and together with the rapid EV isolation platform, the present method may serve as a promising tool for ESCC detection and screening towards clinical translations.

4. Conclusions

ESCC is a global disease that is characterized by local invasion, early metastasis, and drug resistance. There are currently no effective non-invasive biomarkers for the diagnosis of ESCC. The majority of ESCC patients are diagnosed at an advanced stage. This significantly reduces the chance of surgical resection and increases the risk of postoperative recurrence. Our study investigated the unique abundance of EV proteins between ESCC patients and healthy controls via the integration of EXODUS and ELISA for ESCC fast detection and screening. We analyzed these proteins and their involvement in pathways related to the

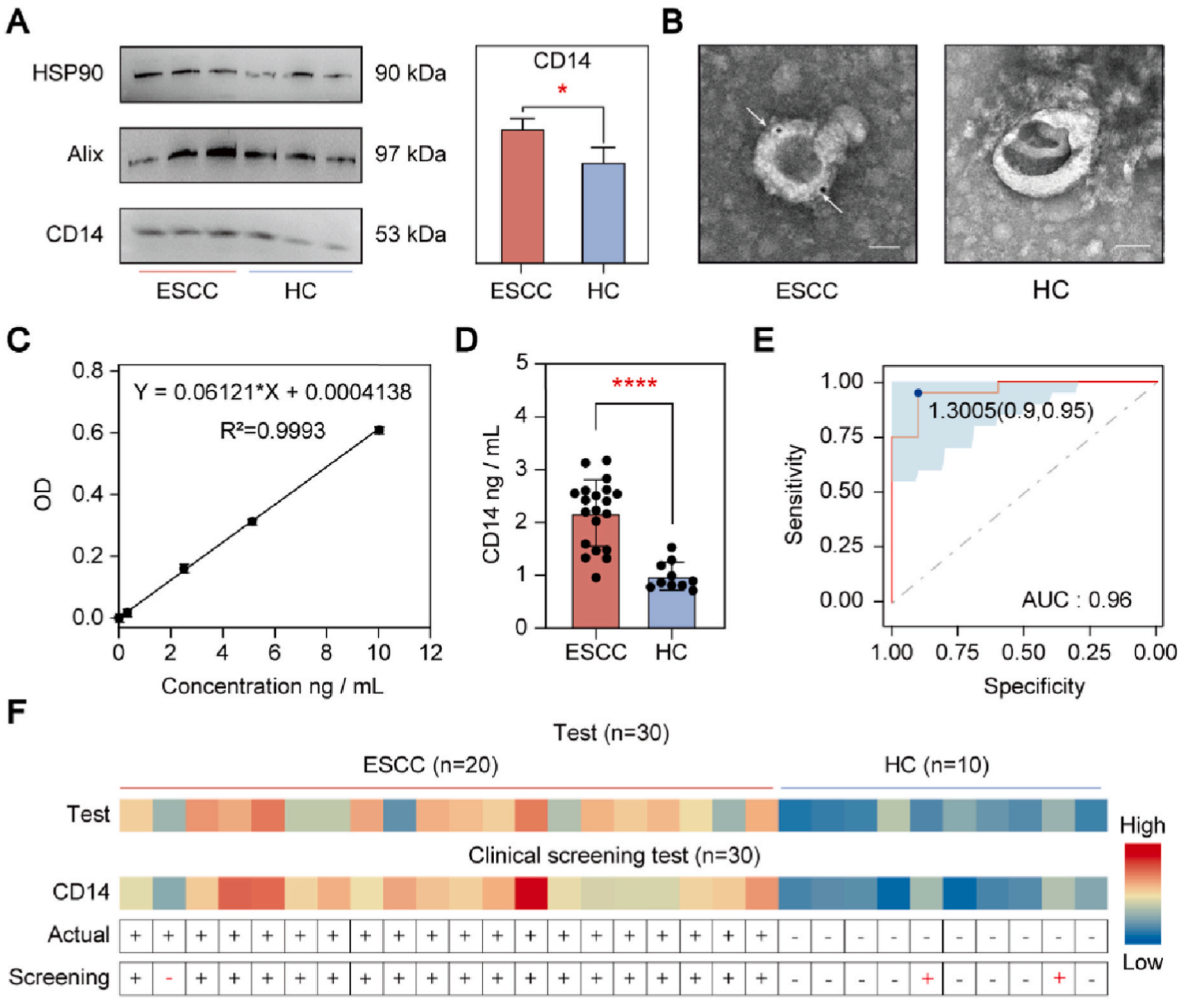

Fig. 4. Validation of differential expression levels of CD14 in ESCC. (A) Expression levels of EV CD14 were determined by Western blot analysis in additional samples. (n = 3 for each group. 50 μg protein was loaded per lane). (B) Immunogold-labeled (anti-CD14) electron microscopy analysis of EVs. Arrows indicate 10 nm gold particles. Scale bar, 50 nm. (C) The line chart shows the standard curve of the ELISA experiment. (D) Boxplot showing EV CD14 was highly expressed in ESCC patients compared with healthy controls, $P < 0.001$. (E) ROC curve analysis revealed that the expression level of CD14 can discriminate ESCC patients from healthy controls with an AUC value of 0.96. (F) Diagnostic potency of CD14 for detection of ESCC patients in a screening test with a cutoff concentration at 0.127 ng/mL plasma.

Table 1
Comparing the present method to the existing methods for ESCC diagnosis.

Method	Marker	AUC*	Sensitivity	Specificity	Blood	Non-invasive	Clinical screening	Ref.
EV-ELISA	EV-CD14	0.958	0.950	0.900	Yes	Yes	90%	Our method
AlphaLISA	Stathmin-1	0.94	0.810	0.939	Yes	Yes	81%	Yan et al., (2018)
Metabolomic	Metabolite panel	0.91	0.900	0.900	Yes	Yes	85%	Jin et al., (2014)
Fluorescence molecular endoscopy	GLUT1/2-DG 800CW	0.85	0.800	0.830	No	No	–	Zhao et al., (2021)
16 S rDNA sequencing	Porphyromonas (Pg)	0.599	0.622	0.700	No	Yes	–	(X. Chen et al., 2022)
ELISA	CXCL8 gene	0.751	0.471	0.779	Yes	Yes	62.1%	(H. Chen et al., 2022)
Immunohistochemistry	Biomarker signature $score_{slug}$	0.760	0.770	0.760	No	Yes	*PPV = 79%, *NPV = 73%	Hasan et al., (2022)
ELISA	Anti-SPP1	0.739	0.410	0.870	Yes	Yes	64%	Wang et al., (2022)
ELISA	IGFBP3	0.710	0.382	0.881	Yes	Yes	*PPV = 81%, *NPV = 52%	Luo et al., (2022)
MiRNA sequencing	miR-205–5p	0.770	0.725	0.700	Yes	Yes	–	Kim et al., (2022)
Metabolomics	Metabolite	0.945	0.891	0.910	Yes	Yes	–	Lv et al., (2021)
ELISA	Protein panel	0.945	0.906	0.967	Yes	Yes	–	Liu et al., (2022)
qRT-PCR	miR-1273f	0.793	0.825	0.590	No	Yes	–	Okuda et al., (2021)
Lipidomics	Lipid panel	0.966	0.913	0.870	Yes	Yes	89.1%	Yuan et al., (2021)

*AUC: area under the curve; *PPV: positive predictive value; *NPV: negative predictive value.

development and progression of esophageal cancer. We demonstrated that plasma EV-CD14 is highly related to development of ESCC, which has been identified and validated as a potential diagnostic biomarker for ESCC. We also performed ELISA method to fast screening and detection of ESCC based on the circulating EV-CD14 from 60 clinical samples, which showed high diagnostic potentials towards clinical applications. Additional studies using a large sample size may be performed to further confirm our findings and investigate the underlying mechanism.

Credit author statement

Qingfu Zhu: Methodology, Validation, Investigation, Writing – review & editing. Hao Xu: Methodology, Data creation, Writing – original draft, Writing – review & editing. Liu Huang: Methodology, Data curation, Resources. Jiaxin Luo: Data curation, Writing – review & editing. Hengrui Li: Writing – review & editing. Rui Yang: Writing – review & editing. Xiaoling Liu: Writing – review & editing. Fei Liu: Conceptualization, Supervision, Project administration, Writing – review & editing, Funding acquisition.

Declaration of competing interest

The authors declare that they have no known competing financial interests or personal relationships that could have appeared to influence the work reported in this paper.

Data availability

Data will be made available on request.

Acknowledgments

We thank Tongji Hospital, Tongji Medical College, and Huazhong University of Science and Technology for providing clinical samples for this study. The work was primarily supported by a research fund provided by the Zhejiang Provincial Natural Science Foundation (LY22H120002), the Zhejiang Provincial and Ministry of Health Research Fund for Medical Sciences (WKJ-ZJ-1910), and the Wenzhou Basic Research Projects (Y2020916).

Appendix A. Supplementary data

Supplementary data to this article can be found online at https://doi.org/10.1016/j.bios.2023.115088.

References

Arnold, M., et al., 2020. Gastroenterology 159, 335–349.e15.
Arnold, M., et al., 2019. Lancet Oncol. 20, 1493–1505.
Bray, F., et al., 2018. CA. Cancer J. Clin. 68, 394–424.
Cao, W., et al., 2021. Chin. Med. J. (Engl). 134, 783–791.
Chae, Y.C., et al., 2016. Cancer Cell 30, 257–272.
Cheah, M.T., et al., 2015. Proc. Natl. Acad. Sci. U. S. A 112, 4725–4730.
Chen, H., et al., 2022. Med 58, 1–13.
Chen, X., et al., 2022. Front. Cell. Infect. Microbiol. 12, 1–11.
Chen, Y., et al., 2021. Nat. Methods 18, 212–218.
de Jong, O.G., et al., 2020. Nat. Commun. 11, 1–13.
Fuentes, P., et al., 2020. Nat. Commun. 11, 1–15.
García-Silva, S., et al., 2021. Nat. Cancer 2, 1387–1405.
Gu, H., et al., 2012. Mol. Biol. Rep. 39, 9105–9111.
Hasan, R., et al., 2022. Oncotarget 13, 1020–1032.
He, G., et al., 2022. Mol. Cancer 21, 1–22.
Hu, T., et al., 2021. Trends in Cancer 7, 122–133.
Huang, L., et al., 2019. Cell Death Dis. 10, 513.
Jiao, Z., et al., 2020. Aging (Albany NY) 12, 15002–15010.
Jin, H., et al., 2014. J. Proteome Res. 13, 4091–4103.
Jordan, et al., 2020. Breast Cancer Res. 22, 1–16.
Kim, S., et al., 2022. J. Clin. Med. 11.
Kumar, A., Deep, G., 2020. Cancer Lett. 479, 23–30.
Labelle, M., et al., 2011. Cancer Cell 20, 576–590.
LeBleu, V.S., Kalluri, R., 2020. Trends in Cancer 6, 767–774.
Li, K., et al., 2022. Mol. Cancer 1–13.
Li, X., et al., 2021. Small Methods 5, 1–11.
Li, Y.-J., et al., 2021. J. Nanobiotechnol. 19, 1–20.
Liu, W., et al., 2022. Clin. Proteonomics 19, 1–17.
Lu, Y., et al., 2020. Cell 180, 1081–1097.e24.
Luo, Y., et al., 2022. Ann. Med. 54, 2153–2166.
Lv, J., et al., 2021. AClin. Transl. Med. 11, 1–6.
Markar, S.R., et al., 2018. JAMA Oncol. 4, 970–976.
Martínez-Reyes, I., Chandel, N.S., 2021. Nat. Rev. Cancer 21, 669–680.
Min, L., et al., 2021. Adv. Sci. 8, e2102789.
Nyrén, O., Adami, H.O., 2009. Textb. Cancer Epidemiol. 2241–2252.
Ohashi, S., et al., 2015. Recent Gastroenterology 149, 1700–1715.
Okuda, Y., et al., 2021. Sci. Rep. 11, 1–10.
Pan, Y., et al., 2021. Trends Pharmacol. Sci. 42, 268–282.
Paolino, G., et al., 2021. Cancers 13, 4157.
Pei, C., et al., 2020. Angew. Chem. Int. Ed. 59, 10831–10835.
Qiu, M., et al. 2020. 10, 5412–5418.
Ramirez-Garrastacho, M., et al., 2021. Br. J. Cancer 126, 331–350.
Reeh, M., et al., 2015. Ann. Surg. 261, 1124–1130.
Song, G., et al., 2017. Oncotarget 8, 17771–17784.
Su, H., et al., 2021. Adv. Mater. 33, 1–12.
Tanaka, Y., et al., 2013. Cancer 119, 1159–1167.
Théry, C., et al., 2018. J. Extracell. Vesicles 7, 1535750.
Thienpont, B., et al., 2016. Nature 537, 63–68.
Wang, C., et al., 2022. BMC Cancer 22, 932.
Xie, Y., et al., 2021. Stem Cell. Int., 2229477, 2021.
Xu, J., et al., 2020. J. Exp. Clin. Cancer Res. 39, 1–15.
Yan, L., et al., 2018. Cancer Med. 7, 1802–1813.
Yuan, Y., et al., 2021. Br. J. Cancer 125, 351–357.
Zhang, Y., et al., 2020. Cancer Res. 80, 3345–3358.
Zhao, X., et al., 2021. Int. J. Mol. Sci. 22, 1–16.
Zhu, Q., et al., 2021. Nanoscale 13, 16457–16464.